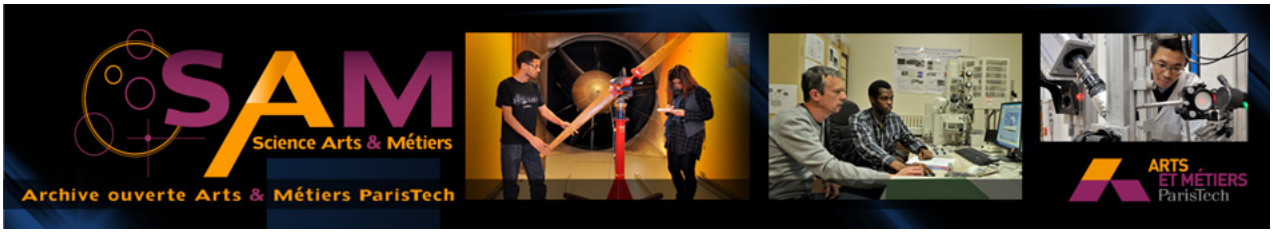

Modelling the effects of wood cambial age on the effective modulus of elasticity of poplar laminated veneer lumber

Abstract.
Key message: A modelling method is proposed to highlight the effect of cambial age on the effective modulus of elasticity of laminated veneer lumber (LVL) according to bending direction and veneer thickness. This approach is relevant for industrial purposes in order to optimize the performance of LVL products.
Context: LVL is used increasingly in structural applications. It is obtained from a peeling process, where product's properties depend on cambial age, hence depend on radial position in the log.
Aim: This study aims to highlight how radial variations of properties and cambial age impacts the mechanical behaviour of LVL panels.
Method: An analytical mechanical model has been designed to predict the modulus of elasticity of samples made from poplar LVL panels. The originality of the model resides in the integration of different data from the literature dealing with the variation in wood properties along the radius of the log. The simulation of the peeling process leads to veneers with different mechanical properties, which are randomly assembled in LVL panels.
Results: The model shows a correct mechanical behaviour prediction in comparison with experimental results of the literature, in particular with the decrease in MOE in LVL made of juvenile wood. It highlights that the bending direction and veneer thickness have no influence on the average MOE, but affect MOE dispersion.
Conclusion: This paper proposed an adequate model to predict mechanical behaviour in the elastic domain of LVL panels based on the properties of raw wood material.

Keywords: Populus, Juvenile wood, Mature wood, Laminated Veneer Lumber

1 Introduction

Laminated veneer lumber (LVL) is an engineering wood product made from veneer sheets glued together layer by layer to form panels or beams. Veneers are mainly obtained from a rotary peeling process which consists in peeling a log from the outside to the core. Peeling lines are computer-controlled, providing access to different types of data from the logs (Thibaut et al. 2015). Significant progresses in wood mechanical behaviour knowledge are needed to manage these log properties into a LVL model.

Furthermore, mechanical properties of LVL are strongly dependent on the mechanical properties of each layer. Juvenile wood is the name given to wood created at the beginning of the radial growth, hence in a zone close to the pith. Juvenile wood usually has a lower density and less mechanical properties than mature wood.

The rotary peeling process can easily separate mature wood from juvenile wood by sorting the veneers by their radial position. However, the impact of juvenile wood on LVL is difficult to apprehend experimentally (Burdurlu et al. 2007), due to the many factors which have an effect on mechanical properties during timber growth cycles. In this work, a model is proposed which considers the impact of juvenile and mature wood, i.e. cambial age. The study focuses on poplar wood species which are typically used in peeling and present fast growth, thus a high ratio of juvenile wood. This study is based on poplar wood properties in general, but principally on the measurements of Rahayu et al.(2014), who studied several poplar cultivars: A4A, Alcinde, Brenta, Dvina, I-214, Koster, Lambro, Lena, Mella, Polargo, Soligo, Taro, Trichobel, Triplo. The model developed is also based on numerous measured properties from the literature (Bao et al. 2001, Fang et al. 2006, Bjurhager et al. 2008, Bremaud et al. 2013, Hein et al. 2013).

The aim is to obtain the behaviour of LVL structural elements (estimation of the modulus of elasticity) from the pith to the bark of an average tree considering different peeling scenarios. In order to achieve this, a representative log is virtually peeled and veneer sheets are sorted according to their category: juvenile or mature wood. Finally, juvenile and mature wood test specimens are reconstituted from each group and simulation results are compared to experimental values from Rahayu et al. (2014).

2 Assessment of mechanical properties variations with cambial age

The longitudinal elastic modulus of wood is influenced by many parameters from the micro to the macro scale, such as Micro Fibril Angle (MFA), density and humidity (Cousins 1976, Cave and Walker 1994, Evans et al. 2000, Evans and Ilic 2001). The material's humidity is not studied here because it is managed during manufacturing due to adhesive process requirements.

As a first step, this study focuses on three main parameters, which are MFA, annual growth ring width and specific gravity. Their variations according to cambial age are taken into account in the model by interpolating experimental data of the literature. As described below, when authors didn't fit their measurements of the properties, a sigmoid function has been fitted on their values. Sigmoid functions allow both to smooth experimental data and provide monotonous curves which have an asymptotic behaviour at the boundary of the measurements.

2.1 Density

Wood density is an important quality attribute, related to many properties like stiffness and strength. Wood density is highly variable due to genetic, environmental, or silvicultural management. As a result, the specific gravity varies throughout the life of the tree.

The following specific gravity data (**Fig. 1**) come from Paillassa et al. (2013) where 14 cultivars were analysed. Each cultivar was characterized using 3 logs of 7 meters

long from 3 different trees. Cultivars had an average density of 330kg.m^{-3}. Wood density at 12% moisture content was calculated for each wood sample per cambial age. **Fig. 1** shows the average specific gravity based on cambial age.

For modelling purposes, a sum of sigmoid function (Eq. (1)) was fitted by using Mathematica fitting method to the experimental values:

$$\rho(C_a) = 319.99 + \frac{37.46}{1 + e^{-1.848(C_a - 14.11)}} + \frac{40.31}{1 + e^{0.8703(C_a - 2.574)}} \tag{1}$$

where specific gravity (ρ in kg.m^{-3}) is predicted from cambial age (C_a in years).

The fitted density variation profile observed in Fig. 1 is comparable to the results proposed by Senft and Bendtsen (1986) for poplar species (Popuplus Deltoid). The specific gravity decreases during the very first years of the tree's life before stabilization. Then it starts to increase from 10 to 16 years old. The density then seems to reach a new threshold, but the data available in the literature are limited for old poplars, entailing lower accuracy in this range. As observed for Larch, Douglas-fir and Scots Pine in literature (Karlman et al. 2005, Filipescu et al. 2013), the specific gravity reaches a horizontal asymptote after a few decades (17 years on average for the studied poplar cultivars), which is obtained thanks to sigmoid functions of Eq. (1).

2.2 Micro fibril angle

MFA is an inherent property at the wood cell level, where wood compounds have a privileged direction due to growing conditions. MFA variation can depend on cambial age (Cave and Walker 1994). **Fig. 2** shows the average MFA with respect to cambial age for seven poplar clones, obtained from an experimental study (Fang et al. 2006). A sum of sigmoid function (Eq. (2)) was fitted to the experimental values (extract from their article), for modelling purposes:

$$MFA(C_a) = 25.82 - \frac{40.30}{1 + e^{-0.3947(C_a - 2.187)}} + \frac{25.81}{1 + e^{-1.202(C_a - 1.542)}} \tag{2}$$

where the MFA (in degrees) is predicted from cambial age (C_a in years). After 12 years, the MFA fitted by the sigmoid function reaches a constant value.

2.3 Specific Modulus of Elasticity

According to Bremaud et al. (2013), there exists a strong relationship between the dynamic specific modulus of elasticity and the MFA. Here we use this relationship, which has been successfully tested for several softwood species (Bendtsen 1986, Reiterer et al. 1999, Sedighi-Gilani et al. 2005). Indeed, poplar is usually classified with softwoods in terms of its mechanical properties. A trigonometric function (Eq. (3)) was fitted by Bremaud et al. (2013) to their experimental values:

$$\frac{E}{\rho}(MFA) = \frac{1}{0.03426\text{Cos}[MFA]^4 + 0.2053\text{Cos}[MFA]^2\text{Sin}[MFA]^2 + 0.6797\text{Sin}[MFA]^4} \quad (3)$$

where the specific modulus (E/ρ inMPa.m^2.kg^{-1}) is predicted from the MFA (in degrees).

The above relationships will enable us to obtain the modulus of elasticity according to the radial position in the log.

2.4 Annual growth ring width

As well as specific gravity, environmental factors affect the width of each annual growth ring. The widths of the growth rings obtained in the study of Paillassa et al. (2013) are presented in **Fig. 4** with respect to cambial age. A sigmoid function (Eq. (4)) was fitted to the experimental values for smoothing purposes:

$$w_{ring}(C_a) = -1.026 - \frac{18.77}{1 + e^{-0.3475(C_a - 6.727)}} + \frac{25.90}{1 + e^{-1.696(C_a - 1.285)}} \quad (4)$$

where the average annual growth ring width (w_{ring} in mm/year) is predicted from the cambial age (C_a in integer years). The average annual growth ring width is supposed to tend to a constant value after 16 years. This hypothesis for normal wood can be observed for other species in literature (Adamopoulos et al. 2010, Guller et al. 2012, Campelo et al. 2015). Notice that for this study, the model will not be used for trees older than 16 years old.

The radius based on cambial age is then deduced by integrating the annual growth ring width for each year of growth (Eq. (4)), with the assumption of a constant growth rate for a given year (cf. **Fig. 4**). This enables us to link the equations based on cambial age to equations based on the log radius:

$$r(\text{C}_\text{a}) = \int_0^{\text{C}_\text{a}} \overline{w_{ring}}(\text{y})dy \qquad \text{with } \overline{w_{ring}}(y) = w_{ring}(C_a) \text{ for } y \in]C_a - 1, C_a] \quad (5)$$

where the radius (r in mm) of the log is determined from the ring width ($\overline{w_{ring}}$ in mm.year^{-1}).

3 Model building

The model was developed using Wolfram Mathematica Software (2015). The model consists of four different phases, detailed in **Fig. 5**. First step is to determine the modulus of elasticity along the generatrix curve of the peeling process using the equations above (Eq. (1) to (5)). The second step is to divide the virtual peeling into sheets and

sort them into two groups, “juvenile” and “mature”. The chosen width of the sheets is 500mm, based on the experimental work of Rahayu et al. (2014). The juvenile and mature groups were defined by their average age, calculated from the annual growth ring width which they originated from. The age threshold between mature and juvenile wood was chosen as 10.6 years, which corresponds to the measured average experimental value in the study of Rahayu et al. (2014). Each sheet is virtually subdivided into n_s subsamples of 20 mm width (the final width of the test specimens). In the third step, for each group the sheets are assembled into n_l layers to represent a LVL panel of 21 mm thickness. The number of constituent panel layers depends on the thickness of the sheets. Sheet thicknesses of 3 mm and 5.25 mm were used, leading to seven layers for the 3 mm sheets and four layers for the 5.25 mm sheets. In this work, it is assumed that sheets can be randomly assembled upside down or not, and the layering is also randomised into a group. Finally, in the last step of the model, the panels are cut into test specimens of 20 mm in width. Then the effective modulus of elasticity of each test specimen is calculated from each layer’s properties as described below.

3.1 Virtual peeling

The first step is to determine the maximum ribbon length depending on the log diameter. In cross-section, the peeling process corresponds to following a spiral curve (**Fig. 5**). The equation of a spiral in polar coordinates is given by Eq. (6), where r_s is the spiral radius (mm) with respect to the angle θ (in rad), r_i is the initial log radius (in mm) and t is the peeling thickness (in mm).

$$r_s(\theta, t) = r_i - t \cdot \frac{\theta}{2\,\pi} \tag{6}$$

The length of this curve can be calculated by the integration of Eq. (6), which corresponds to the ribbon length. Second-order length is neglected due to linear variations in radius with respect to the angle. Thus the ribbon length from the core is determined by the following equation (7):

$$l(r_i, r_f, t) = \int_{2\pi\cdot\frac{r_f}{t}}^{2\pi\cdot\frac{r_i}{t}} \sqrt{\frac{\partial r_s(\theta,t)}{\partial\theta}^2 + r_s(\theta,t)^2}\, d\theta \tag{7}$$

Where l (in mm) is the ribbon length from the core and r_f (in mm) the final log radius.

The integration domain depends on both the final and the initial log radius. Indeed, logs are not peeled up to the log centre; there remains a peeler core of r_f radius. Initial and final log radii were chosen to be respectively 200 and 35 mm for comparison purposes with the study of Rahayu et al. (2014).

3.2 Mechanical properties computation

Using the above equations (Eq. (1) to (7)) taken from the literature, it is then possible to determine the wood's modulus of elasticity along the peeling sheet by composing them (Eq. (8)) to obtain parametric coordinates on cambial age basis:

$$\begin{cases} l &= l\big(r_i(C_a,t), r_f, t\big) \\ E &= \frac{E}{\rho}\big(\mathrm{MFA}(C_a)\big).\rho(C_a) \end{cases} \tag{8}$$

Where l (in mm) is the ribbon length from the core and E (in MPa) is the modulus of elasticity. These values are parametrized by the cambial age (Ca).

In **Fig. 6**, solid lines represent some examples for different peeling thicknesses showing the modulus of elasticity with respect to ribbon length for an initial log radius of 200 mm and a kernel log radius of 35 mm. Because of the 35 mm kernel radius, the model does not no use any extrapolated value towards the centre of the logs. Indeed, 35 mm radius corresponds to a cambial age higher than 3 years old, and all data in use starts to 1 year old.

Values beyond 200 mm radius are shown in dashed line in **Fig. 6**. These values are almost constant due to the asymptotic behaviour of sigmoid curves, but they are not used in the model. However, if the model were used beyond 200 mm, the extrapolation would not produce outliners due to sigmoid function property.

3.3 Calculation of Flatwise and Edgewise modulus of elasticity

Since the modulus of elasticity varies into each layer of each panel, it is necessary to compute an effective modulus of elasticity for each test specimen. The effective modulus of elasticity corresponds to the apparent modulus of elasticity for an equal and homogenous section. Moreover, this modulus of elasticity depends on the loading direction, because the impact of each layer on the mechanical behaviour of the LVL is different in flatwise or edgewise configuration (Burdurlu et al. 2007). This will be discussed in the next paragraph. In the model, the interface connection stiffness is considered higher than the material's raw stiffness. This is a prerogative in European standard (EN 14374) concerning LVL panels.

Edgewise

In an edgewise bending test, each layer can be considered as independent. Thus, the effective modulus of elasticity is determined by calculating the sum of the stiffness of each layer, as in the following Eq. (9), according to Voigt principle:

$$(E)_e = \frac{\sum_{i=1}^{n_l} E_i I_i}{I_t} \tag{9}$$

With:

E_i	Modulus of elasticity of the ith layer	MPa
I_i	Local inertia of the ith layer	mm^4
I_t	Inertia of the homogeneous section	mm^4
n_l	number of layer	–

Flatwise

In a flatwise bending test, the location of layers with different mechanical properties has more influence on global properties than in an edgewise bending test, due to a different stress rate between border and central layers. To calculate the effective modulus of elasticity in the flatwise direction, the position of neutral section axis has first to be determined thanks to the following equation (10) (cf. **Fig. 7**):

$$z_0 = \frac{\sum_{i=1}^{n_l} z_{0,i} E_i S_i}{\sum_{i=1}^{n_l} E_i S_i} \tag{10}$$

With, in accordance with **Fig. 7**:

z_0	Distance from the neutral axis to an arbitrary reference	mm
$z_{0,i}$	Distance from the ith layer neutral axis to an arbitrary reference	mm
z_i	Distance from the ith layer neutral axis to the global neutral axis	mm

Thus, the distance between each layer's neutral axis and the global neutral axis, z_i is deduced by equation (11):

$$z_i = z_{0,i} - z_0 \tag{11}$$

Then, the effective modulus of elasticity can be determined by the following Eq. (12), according to Steiner's principle:

$$(E)_f = \frac{\sum_{i=1}^{n_l} E_i I_i + S_i z_i^2}{I_t} \tag{12}$$

With:

E_i	Modulus of elasticity of the ith layer	MPa
I_i	Inertia of the ith layer	mm^4
I_t	Inertia of the whole section	mm^4
S_i	Section of the ith layer	mm^2
z_i	Distance from the ith layer neutral axis to the neutral axis	mm

3.4 Stochastic approach

As each virtual peeling process is based on a randomised assembly process, the process is repeated a thousand times to identify and enhance a tendency. Indeed, the peeling process always gives the same veneer for a given thickness value, but there are several combinations of sheet arrangements after the primary cutting. These combinations are also increased by including the possibility to turn each sheet upside-down. For a given set of veneer sheets, the sheet positioning influences the flatwise modulus of elasticity, whereas it does not impact the edgewise modulus of elasticity. Consequently, a great number of processes have to be performed to obtain results close to experimental conditions. The number of possible combinations for a single n_l layer LVL is given by Eq. (13) below:

$$n_{comb} = \frac{n_l! \cdot 2^{n_l}}{2} \tag{13}$$

Where n_{comb} is the number of possible combinations and n_l is the number of layers. Symmetric cases are considered in the number of combinations; consequently the number is halved.

For the log size used, there are respectively 175 and 250 test specimens per log for respectively juvenile and mature groups. Note that the number of specimens does not depend on veneer thickness, but only on the volume of the test specimens. The number of possible combinations is determined with binomial coefficients, which gives the following results (Eq. (14)) for the studied cases (4 layers of 5.25 mm thickness and 7 layers of 3 mm thickness over a total number of test specimens of 175 or 250):

$$\begin{cases} \binom{175}{4} \approx 3.77 \times 10^{7} \\ \binom{250}{4} \approx 1.58 \times 10^{8} \\ \binom{175}{7} \approx 8.83 \times 10^{11} \\ \binom{250}{7} \approx 1.11 \times 10^{13} \end{cases} \tag{14}$$

Due to the numerous ways to choose n_l sheets from a set of 175 or 250 elements, a stochastic approach is chosen in order to obtain results within a reasonable computing time.

4 Results

The model can be used to predict the effective elastic modulus of a parameterized LVL sample. It could be used with different scenarios but requires validation through a comparison with experimental data, which is done in the following.

4.1 Experimental results

A study of Rahayu et al. (2014) was carried out on ten different poplar species, where juvenile and mature wood LVL had their moduli of elasticity measured. A summary of the results is shown in **Table 1**. The dynamic MOE of LVL composed of juvenile wood appears to be significantly lower than that of mature wood, with a ratio of 0.858. The flatwise MOE is also slightly lower than the edgewise MOE, while there is no significant effect of veneer thickness. According to the authors, the differences in specific gravities are low and cannot alone explain these observations.

4.2 Model results

Our model was computed with the following parameters to fit the experimental set up presented by Rahayu et al. (2014): initial log radius: 200 mm; kernel log radius: 35 mm; sheet thicknesses: 3 and 5.25 mm; sheet length: 500 mm; test sample width: 20 mm; and juvenile cambial age limit: 10.6 years.

Fig. 8 and **Fig. 9** show the distribution of test samples with respect to the modulus of elasticity. Common statistical values are given in **Table 2** and **Table 3**.

As expected in the light of the input parameters, mature groups have a higher average modulus of elasticity value (8225 ± 220 MPa) than juvenile groups (6461 ± 449 MPa) (cf. **Table 2**), which leads to a modulus of elasticity ratio of 0.79 between juvenile and mature groups. Each juvenile group has a higher dispersion than mature groups, which is shown by coefficients of variation from 5.03 up to 8.86% for juvenile groups and only from 1.94 to 3.35% for mature groups.

The dispersion of modulus of elasticity is higher in a flatwise configuration than in an edgewise configuration, due to the greater influence of border layers in flatwise cases. Dispersion also increases between 3 mm and 5.25 mm LVL thicknesses because of the number of layers used. Indeed, the fewer layers there are, the greater influence they have.

A comparison between experimental and model MOE values can be made thanks to **Table 1** and **Table 2**, where the measurements are classified into groups according to whether the wood is juvenile or mature, and sheet thicknesses (3 and 5.25 mm). The comparison shows that modelled MOE are systematically lower than experimental ones, and that the standard deviation is higher for the experimental data.

Juvenile LVL shows a significantly lower MOE in both the model and experimental results. No clear effect of the veneer thickness or the loading direction appears in the model, while in the experimental results there is no significant effect of veneer thickness, but a statistically significant effect of loading direction on the dynamic MOE exists. Nevertheless, this effect appears non-existent when looking at the static MOE, showing that this result has to be discussed (contrary to the effect of juvenility).

5 Discussion

The model is based on the assumption that all poplar trees and cultivars behave in the same way in terms of growth, MFA variation and juvenile – mature transition, and

thus the coefficient of variation (6.95 and 2.67%) is obviously lower than in the experimental results from (around 15% regardless of the group).

The experimental ratio between the dynamic MOE of juvenile and mature wood is 0.876, which is higher than the model prediction (0.785). However, the results of Rahayu et al. (2014) present a higher coefficient of variation (**Table 1**). The study's ratio is included between 0.69 and 1.06 by considering both standard deviations of juvenile and mature modulus of elasticity. Indeed, uncertainty of a ratio can be calculated from the standard deviation of each part of this ratio. Therefore the results obtained with the model are close or similar to those from Rahayu et al. (2014). However, several reasons could have induced different ratios. From the experimental point of view, there exist difficulties in distinguishing juvenile from mature wood in Rahayu et al. (2014). Indeed, groups were made by visual observation of false heartwood but false heartwood does not necessarily correspond exactly to juvenile wood. Furthermore, a part of the studied logs was quite young, with a first quartile equal to 13.25 years, which leads to a minor number of mature annual growth rings to obtain a reliable long term evolution of mature wood properties. From the modelling point of view, there is a lack of experimental input data for mature wood in the literature (Thibaut et al. 2015), entailing an assumption of steady parameters for extra dataset domain for raw material properties. By doing so, the MOE of mature wood is bounded in the model, and the dispersion of LVL composed of mature wood is very low in comparison with experimental measurements. Thus the MOE can be underestimated, especially for mature wood, leading to the higher ratio between the juvenile and mature wood MOE observed in the model.

Despite the observed differences between experimental and modelled MOE values, this study takes the stand of not modifying experimental values from the literature to obtain a first model without entering modifications. In this way, it is easier to understand the influence of each property's behaviour without any behaviour correction. The difference can rely on the relationship between the specific modulus and MFA (**Fig. 3**) based on Bremaud et al. (2013). These experimental results show a significant dispersion in the ten to twenty degrees range. Furthermore, they were performed on a coniferous tree, which shows similar mechanical properties to populus, but poplar has a different internal structural anatomy, like a broad-leaved tree. In Rahayu et al. (2014), the effect of thickness and bending direction cannot be concluded, since dynamic and static MOE give contrary results. Indeed, dynamic MOE results show an influence of bending direction but not of thickness, whereas static MOE results give the opposite conclusion. Modelling shows no influence from either thickness or bending direction on the average MOE. However, compared to edgewise bending, the model shows an increase in standard deviation for flatwise bending, as well as for 5-layer LVL compared to 3-layer LVL.

The results obtained by Rahayu et al. (2014) indicate that maturity is a source of variance of the effective modulus of elasticity after performing an ANOVA test on the dynamic and static test results; this variance also occurs with the model.

6 Conclusion

The paper proposes a modelling method to predict LVL elastic behaviour. This model is based on experimental measurements to create an average poplar log, which is used in a simulated peeling process. This study shows a correct mechanical behaviour prediction by the developed model compared to experimentally determined behaviour from Rahayu et al. (2014), in particular with the decrease in MOE in LVL made of juvenile wood. The model, featuring a stochastic approach, is also able to predict LVL behaviour according to veneer thickness and loading direction. Indeed, model results show no influence of these parameters on the average MOE. However, the model shows that dispersion is higher for flatwise than for edgewise bending. Greater veneer thickness also increases the dispersion. Model accuracy could be improved by leading a measurement campaign to determine a reliable specific modulus of elasticity for poplar cultivar. Indeed, this study relies on a softwood specific modulus of elasticity and could underestimate the specific MOE value on poplar with respect to specific gravity.

From a practical perspective, this model could be used to highlight the necessity or not of sorting veneer sheets in an industrial process by showing the impact of juvenile wood in LVL products. It could also help to estimate the impact of a peeling strategy to build LVL billets as regards veneer thickness.

Acknowledgment

This research was carried out at the Laboratoire Bourgogne des Matériaux et des Procédés (LaBoMaP), Ecole National Superieure d'Arts et Métiers (ENSAM), Cluny, Bourgogne, France. We wish to thank our partners FCBA (especially Alain Berthelot who perform physical analysis of poplar samples) and CNPF IDF for their active collaboration on this large research program. We also wish to thank our partners and funders of the Xylomat Technical Platform from the Xylomat Scientific Network funded by ANR-10-EQPX-16 XYLOFOREST.

References

Adamopoulos, S., C. Passialis and E. Voulgaridis (2010). "Ring width, latewood proportion and density relationships in black locust wood of different origins and clones." IAWA journal **31**(2): 169-178.

Bao, F., Z. Jiang, X. Jiang, X. Lu, X. Luo and S. Zhang (2001). "Differences in wood properties between juvenile wood and mature wood in 10 species grown in China." Wood Sci. Technol. **35**(4): 363-375.

Bendtsen, B. (1986). "Mechanical and anatomical properties in individual growth rings of plantation-grown eastern cotton-wood and loblolly pine." Wood Fiber Sci **18**: 23-38.

Bjurhager, I., L. A. Berglund, S. L. Bardage and B. Sundberg (2008). "Mechanical characterization of juvenile European aspen (Populus tremula) and hybrid aspen

(Populus tremula Populus tremuloides) using full-field strain measurements." J. Wood Sci. **54**(5): 349-355.
Bremaud, I., J. Ruelle, A. Thibaut and B. Thibaut (2013). "Changes in viscoelastic vibrational properties between compression and normal wood: roles of microfibril angle and of lignin." Holzforschung.
Burdurlu, E., M. Kilic, A. C. Ilce and O. Uzunkavak (2007). "The effects of ply organization and loading direction on bending strength and modulus of elasticity in laminated veneer lumber (LVL) obtained from beech (Fagus orientalis L.) and lombardy poplar (Populus nigra L.)." Constr. Build. Mater. **21**(8): 1720-1725.
Campelo, F., J. Vieira, G. Battipaglia, M. de Luis, C. Nabais, H. Freitas and P. Cherubini (2015). "Which matters most for the formation of intra-annual density fluctuations in Pinus pinaster: age or size?" Trees **29**(1): 237-245.
Cave, I. and J. Walker (1994). "Stiffness of wood in fast-grown plantation softwoods: the influence of microfibril angle." For. Prod. J. **44**(5): 43.
Cousins, W. (1976). "Elastic modulus of lignin as related to moisture content." Wood Sci. Technol. **10**(1): 9-17.
Evans, R. and J. Ilic (2001). "Rapid prediction of wood stiffness from microfibril angle and density." For. Prod. J. **51**(3): 53.
Evans, R., J. Ilic, C. Matheson, L. Schimleck, P. Blakemore and others (2000). Rapid estimation of solid wood stiffness using SilviScan. Proceedings of 26th Forest Products Research Conference: Research developments and industrial applications and Wood Waste Forum, Clayton, Victoria, Australia, 19-21 June 2000.
Fang, S., W. Yang and Y. Tian (2006). "Clonal and within-tree variation in microfibril angle in poplar clones." New Forests **31**(3): 373-383.
Filipescu, C. N., E. C. Lowell, R. Koppenaal and A. K. Mitchell (2013). "Modeling regional and climatic variation of wood density and ring width in intensively managed Douglas-fir." Can. J. For. Res. **44**(3): 220-229.
Guller, B., K. Isik and S. Cetinay (2012). "Variations in the radial growth and wood density components in relation to cambial age in 30-year-old Pinus brutia Ten. at two test sites." Trees **26**(3): 975-986.
Hein, P. R. G., J. Silva and L. Brancheriau (2013). "Correlations among microfibril angle, density, modulus of elasticity, modulus of rupture and shrinkage in 6-year-old Eucalyptus urophylla E. grandis." Maderas: Cienc. Tecnol. **15**(2): 171-182.
Karlman, L., T. Mörling and M. Owe (2005). "Wood Density, Annual Ring Width and Latewood Content in Larch and Scots Pine." Eurasian J. For. Res. **8**(2): 91-96.
Paillassa, E., A. Berthelot, D. Reuling, G. Robert, A. Bouvet, J.-D. Lanvin, G. Legrand, J. Moreau and L. Denaud (2013). "Wood quality of new poplar cultivar
" Foret entreprise(213): 16-19.
Paillassa, E., A. Berthelot, D. Reuling, G. Robert, A. Bouvet, J.-D. Lanvin, G. Legrand, J. Moreau and L. Denaud (2013). Wood quality of new poplar cultivar : Final technical report**:** 138p.
Rahayu, I., L. Denaud, R. Marchal and W. Darmawan (2014). "Ten new poplar cultivars provide laminated veneer lumber for structural application." Ann. For. Sci.: 1-11.

Reiterer, A., H. Lichtenegger, S. Tschegg and P. Fratzl (1999). "Experimental evidence for a mechanical function of the cellulose microfibril angle in wood cell walls." Philos. Mag. A **79**(9): 2173-2184.
Sedighi-Gilani, M., H. Sunderland and P. Navi (2005). "Microfibril angle non-uniformities within normal and compression wood tracheids." Wood Sci. Technol. **39**(6): 419-430.
Senft, J. F. and B. A. Bendtsen (1986). Juvenile wood: processing and structural products considerations. Series: Conference Proceedings.
Thibaut, B., L. Denaud, R. Collet, R. Marchal, J. Beauchene, F. Mothe, P.-J. Méausoone, P. Martin, P. Larricq and F. Eyma (2015). "Wood machining with a focus on French research in the last 50 years." Ann. For. Sci.: 1-22.
Wolfram Research, I. (2015). Mathematica, Version 10.2.

7 Tables

Table 1.: The effects of veneer thickness, cultivar, maturity and sample position on static and dynamic MOE and density (measurements from Rahayu et al. (2014))

Group	n	Dynamic MOE (MPa)	Static MOE (MPa)	Density ($kg.m^{-3}$)
3 mm	1203	8707.18±1334.7	8201.54±1333.6	414.58±35.3
5.25 mm	604	8774.34±1551.6	8415.64±1516.1	394.91±39.7
Mature	905	9298.49±1373.7	8879.49±1336.6	408.25±37.3
Juvenile	902	8157.86±1204.8	7664.24±1185.6	401.26±38.4
Flatwise	949	8654.64±1401.8	8267.40±1419.1	407.91±37.8
Edgewise	858	8811.50±1418.1	8278.70±1381.4	408.11±38.2

Table 2. Predicted MOE (MPa) of each group of LVL

Group	n	Min	Max	Average	STD	COV (%)
3mm	238,000	5171	8793	7271	931	12.80
5.25mm	238,000	4837	8819	7254	970	13.38
Juvenile	285,600	4837	7511	6461	449	6.96
Mature	190,400	7649	8819	8225	220	2.67
Edgewise	238,000	5075	8805	7269	927	12.75
Flatwise	238,000	4837	8819	7256	974	13.42

Table 3. Predicted MOE (MPa) of juvenile and mature groups of LVL

Group	Juvenile		Mature	
Thick-ness	3mm	5.25mm	3mm	5.25mm

Type	Edgewise	Flatwise	Edgewise	Flatwise	Edgewise	Flatwise	Edge-wise	Flatwise
n	71,400	71,400	71,400	71,400	47,600	47,600	47,600	47,000
Min	5340	5171	5075	4837	7738	7726	7662	7649
Max	7406	7448	7471	7511	8790	8793	8805	8819
Aver-age	6475	6466	6467	6433	8235	8227	8219	8219
STD	326	436	430	570	160	219	208	275
COV (%)	5.03	6.75	6.65	8.86	1.94	2.66	2.53	3.35

8 Captions of figures

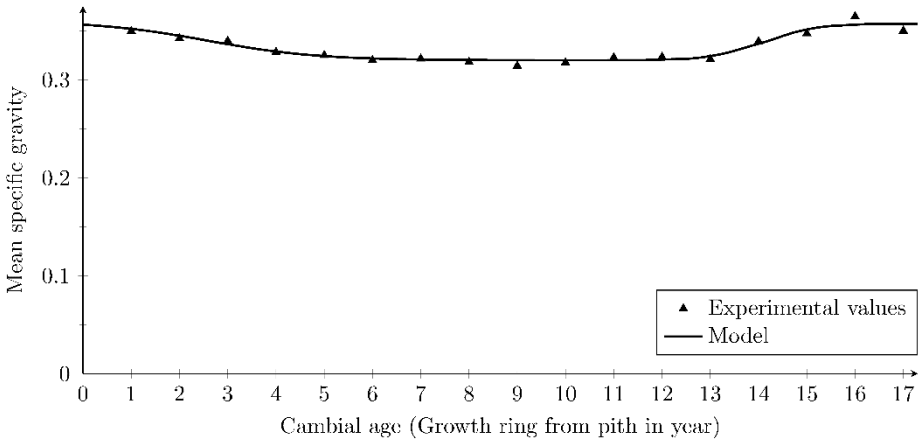

Fig. 1. Variation in specific gravity with cambial age for poplar cultivar (measurements from (Paillassa et al. (2013))

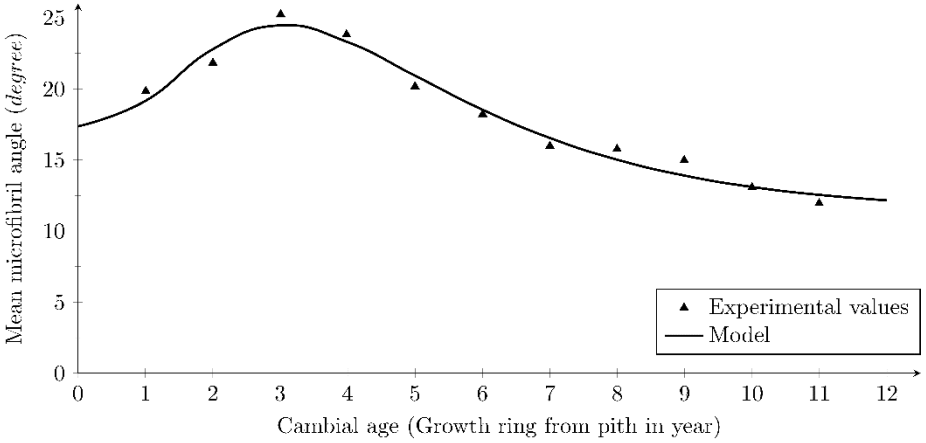

Fig. 2. Variation in MFA with cambial age for seven poplar clones at breast height (measurements from Fang et al. (2006))

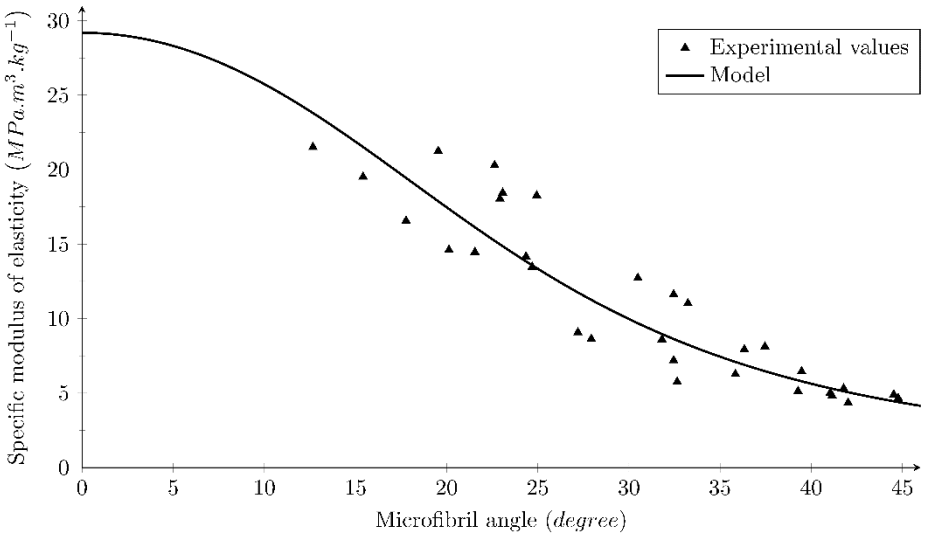

Fig. 3. Variation in dynamic specific modulus of elasticity with MFA (measurements from Bremaud et al. (2013))

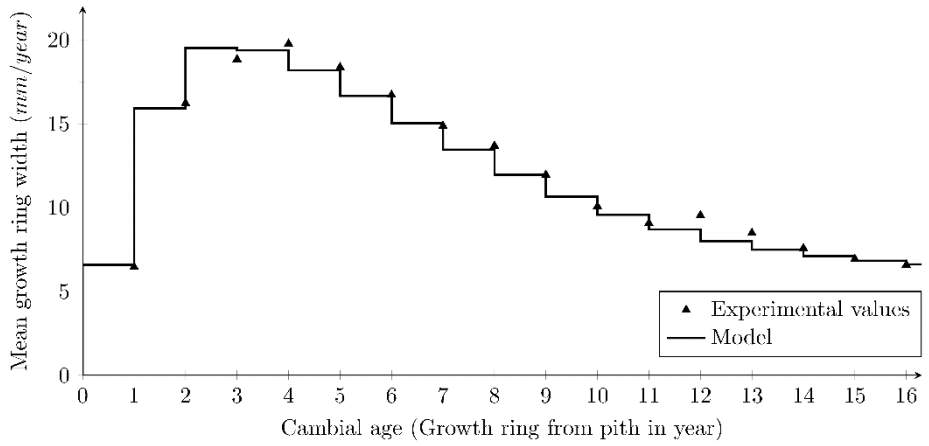

Fig. 4. Variation in average growth ring width with respect to cambial age (measurements from Paillassa et al. (2013))

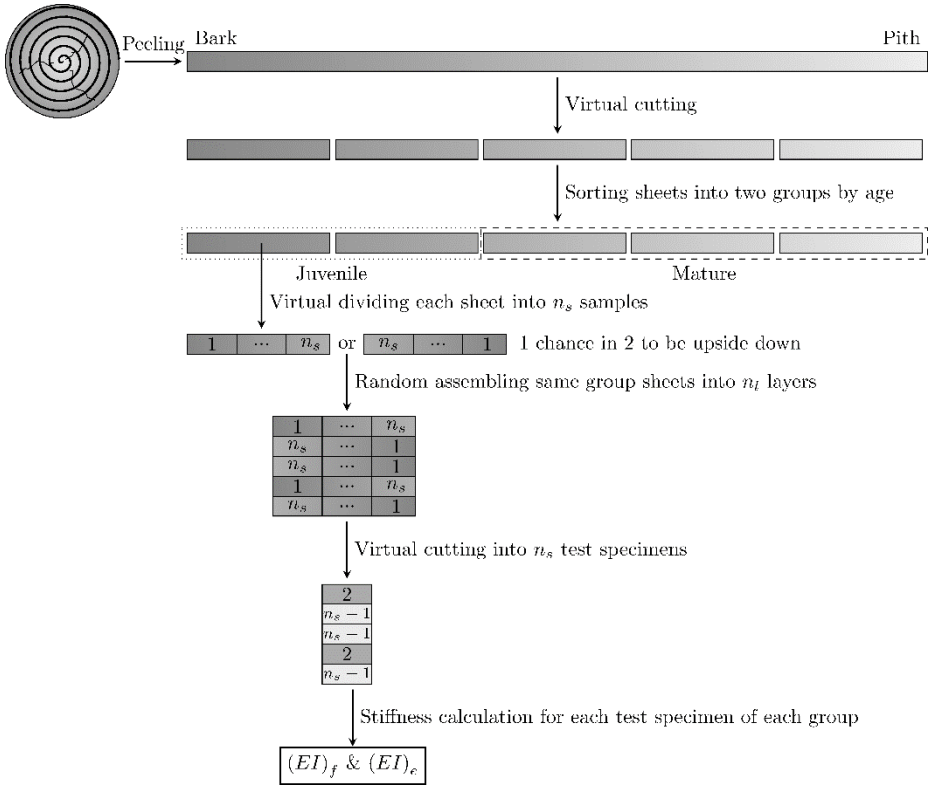

Fig. 5. Virtual peeling and assembly process (shades of grey correspond to local cambial age of sheet)

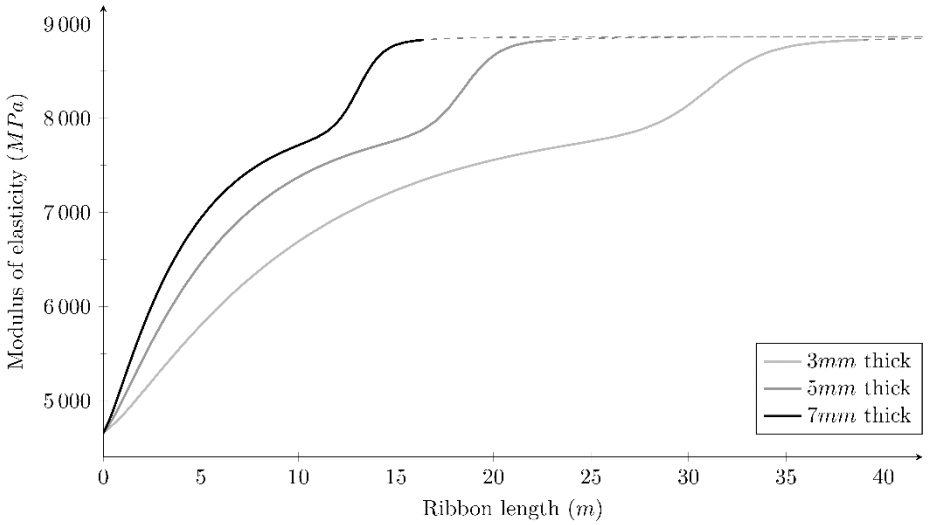

Fig. 6. Examples of modulus of elasticity with respect to ribbon length for different peeling thicknesses (for an initial log radius of 200 mm and a kernel log radius of 35 mm)

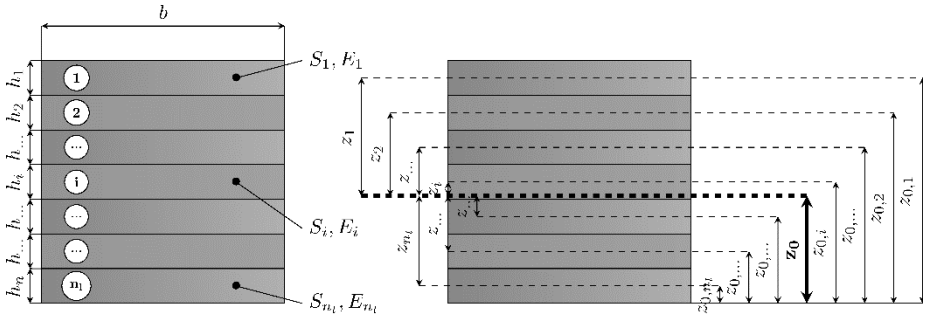

Fig. 7. Geometrical and mechanical properties of LVL in a specimen cross-section

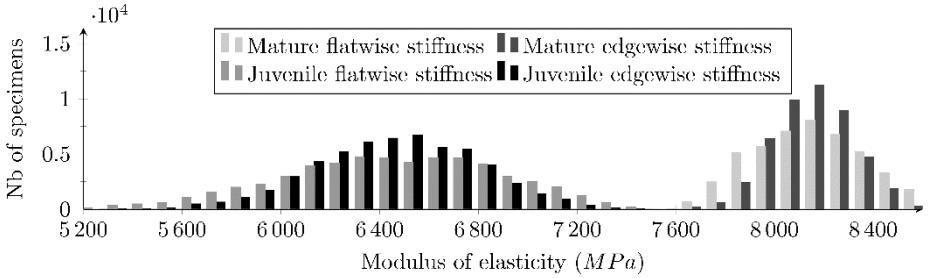

Fig. 8. Predicted test samples of 3mm thick layers

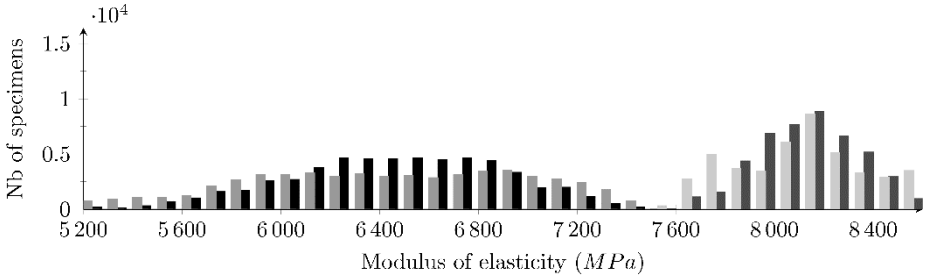

Fig. 9. Predicted test samples of 5.25mm thick layers